

USING A MOBILE RADIO ECHO SOUNDER TO MEASURE BEDROCK TOPOGRAPHY IN EAST QUEEN MAUD LAND, ANTARCTICA

Hideo MAENO¹, Kokichi KAMIYAMA², Teruo FURUKAWA², Okitsugu WATANABE², Renji NARUSE³, Ken'ichi OKAMOTO¹, Takeshi SUITZ¹ and Seiho URATSUKA¹

¹*Communications Research Laboratory, Ministry of Posts and*

Telecommunications, 2-1, Nukui-kitamachi 4-chome, Koganei-shi, Tokyo 184

²*National Institute of Polar Research, 9-10, Kaga 1-chome, Itabashi-ku, Tokyo 173*

³*Institute of Low Temperature Science, Hokkaido University,*

Kita-19, Nishi-8, Kita-ku, Sapporo 060

Abstract: As part of the Dome-Fuji Project, the topography of the bedrock over a wide area around Dome-F and along routes from Dome-F to S16 (about 1000 km distance) was surveyed by radio echo sounder with a continuous recording system. The bedrock topography was successfully measured under ice sheets thicker than 3500 m, and the performance of the radio echo sounder was confirmed. The highest point of Dome-F was located in the basin like topography of the bedrock, surrounded by more elevated areas. The strength of the bedrock echo were found to differ substantially between inside and outside of the Dome-F area. This difference is probably due to the difference of ice sheet temperatures between these areas, because the attenuation coefficients depend on the ice temperature. The stronger echo at high altitude will enable us to measure ice thickness more than 3500 m.

1. Introduction

The 33rd Japanese Antarctic Research Expedition (JARE-33) (November 1991–March 1993) started glaciological and logistic work for a Deep Ice Coring Project at Dome-Fuji, East Antarctica. As part of this project, the bedrock topography was measured by a mobile radio echo sounder from October to December 1992. To measure the ice thickness over the Dome-F area, the sounder system was required to be able to measure more than 3000 m thickness. The information on the bedrock topography will be used to select the exact deep coring point on Dome-F.

The first radio echo sounder measurements around Dome-F were carried out by JARE-26 (AGETA *et al.*, 1985), but the data were obtained only at a few points. Continuous radio echo sounding was successfully carried out near the coastal region by airplane by JARE-27 (URATSUKA *et al.*, 1989; URATSUKA, 1990). During JARE-33, the same sounder was remounted on an oversnow vehicle. The original antenna was replaced by a larger one, and a digital oscilloscope and a laptop computer were used to record data. This system enabled us to measure the ice thickness even when the oversnow vehicle was moving.

This paper describes the radio echo sounding system and the results obtained.

2. System

Figure 1 shows a newly introduced oversnow vehicle (type SM100) with the sounder antenna. This antenna is larger than the original one in the airborne system. Continuous measurements can be carried out after the installation of the antenna on the roof of the vehicle. The sounder uses a bistatic radar system. A two-stack Yagi antenna on one side of the vehicle is used for transmission and the other for receiving. One stack consists of eight elements, resulting in an antenna gain of 12.5 dB. The total antenna gain for transmission and receiving is 16.5 dB. The original antenna for the airborne system was a three-element Yagi antenna with a gain of 8.25 dB.

Table 1 lists the sounder characteristics. The frequency is 179 MHz. One of three pulse lengths (1.0, 0.25, and 0.06 μ s) can be selected. A shorter pulse provides better resolution, and a longer pulse better sensitivity. The longer pulse length is therefore usually chosen for deeper measurements of ice thickness. The pulse repetition frequency is 1 kHz with a peak power of 1 kW.

Figure 2 is a block diagram of the sounder. The pulse modulator generates a pulse-modulated 179 MHz signal after receiving a trigger signal. The pulse-modulated signal is fed to a two-stage solid state amplifier and transmitted from a two-stack Yagi antenna. The return signal is received by the other two-stack Yagi antenna and then fed to an amplifier with a noise level of less than 1 dB. The signal is down-converted to an intermediate frequency of 60 MHz after amplification and attenuation to adjust the signal level.

The intermediate frequency signal is fed to one of the three bandpass filters



Fig. 1. Oversnow vehicle with the antennas of the radio echo sounder on the roof.

Table 1. Major characteristics of the 179 MHz oversnow vehicle radio echo sounder system.

Transmitter	Frequency	179 MHz
	Peak power	1 kW
	Pulse width	60/250/1000 ns
	Resolution in air	9/37.5/150 m
	Resolution in ice ¹	5.1/21.4/85.5 m
	Repetition period	1 ms
Receiver	Sensitivity ²	-110 dBm
	Band width	14/4/1 MHz
	Noise figure	< 1 dB
Antenna	Type	8-element Yagi 4 stack
	Gain	16.5 dBi
	Beam width	20° (in air)
Recording	Digital	3.5-inch floppy disk 2048 byte per min

¹Refractive index of 1.78 is assumed.

²Receiver bandwidth is 4 MHz.

corresponding to the pulse length and then compress by a logarithmic amplifier to increase the dynamic range of the signal to about 70 dB. Nominally, the average is taken over 256 samples. The averaged data are transferred to a laptop computer and recorded on diskettes. To prevent misrecording due to vibration, the data are transferred to the floppy diskettes when the vehicle is stationary.

Before measurements, the radar parameters (such as the range, the averaging number, and the pulse length) are selected according to the observation objectives and estimated ice thickness. The observable range and pulse length are input by switches on the sounder panel. Other parameters such as the averaging number are input through the laptop computer to the oscilloscope.

To monitor the performance at real-time, the computer displays the A-scope and Z-scope images as a quick look. The A-scope image shows the received power *versus* time or range, and the Z-scope image shows the time sequence of the averaged differentiated received power by time.

Figure 3 shows an example of an A-scope image. When a 1- μ s pulse is used, the return signal is masked by the transmission pulse up to a range of about 100 m. If the ice thickness is less than 200 m, the return signal is so strong that the receiver becomes saturated. The power received from the internal layers deeper than about 2000 m is so weak that it is masked by the noise. The return signal from the bedrock surface is much stronger than the signal from the internal layers in the ice sheet, and the return signal clearly appears even when the ice depth is about 3000 m.

Figure 4 shows an example of a Z-scope image. The abscissa indicates the serial number of the observation time. The bedrock topography along the

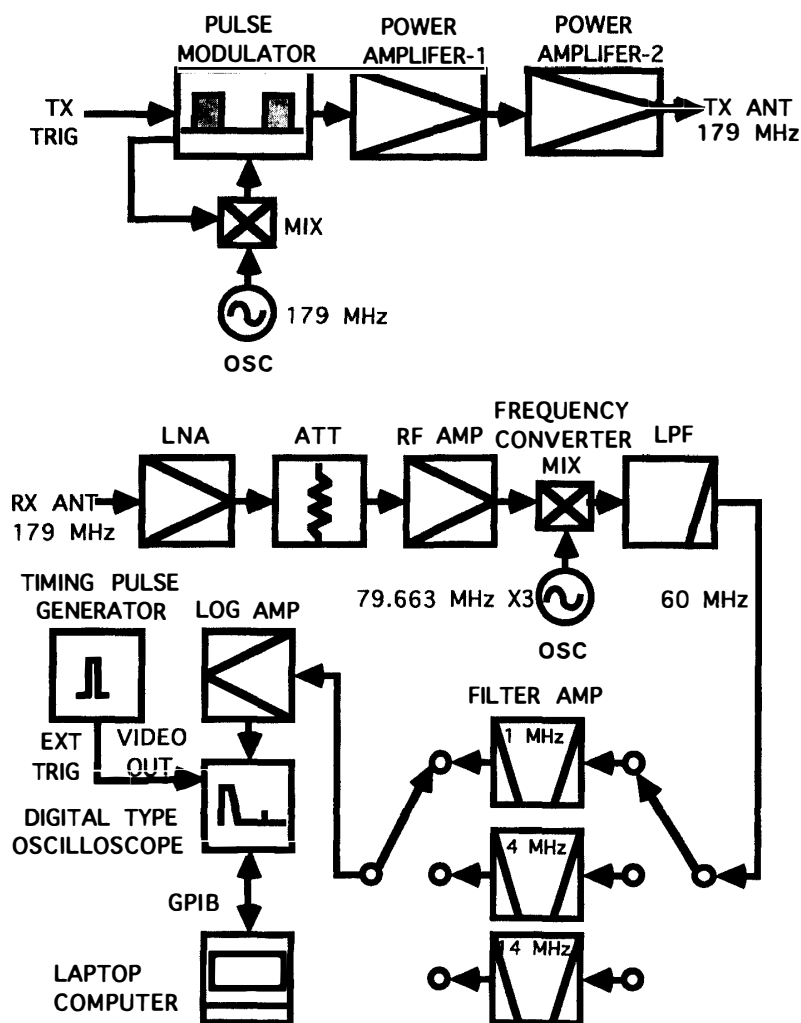


Fig. 2. Block diagram of the radio echo sounder.

oversnow vehicle route was obtained by operating the sounder continuously while the oversnow vehicle was moving. If the oversnow vehicle stopped, the echoes collected in this method appear as parallel straight lines in the figure. The Z-scope image is useful to investigate the bedrock topography and the internal layers.

In Figs. 3 and 4, the ice thickness range was determined by the delay time from the pulse transmission to reception as

$$d = (c \tau / 2) (1/1.78),$$

where c is the velocity of light in vacuum and τ the delay time. The constant 1.78 is a typical refractive index of ice.

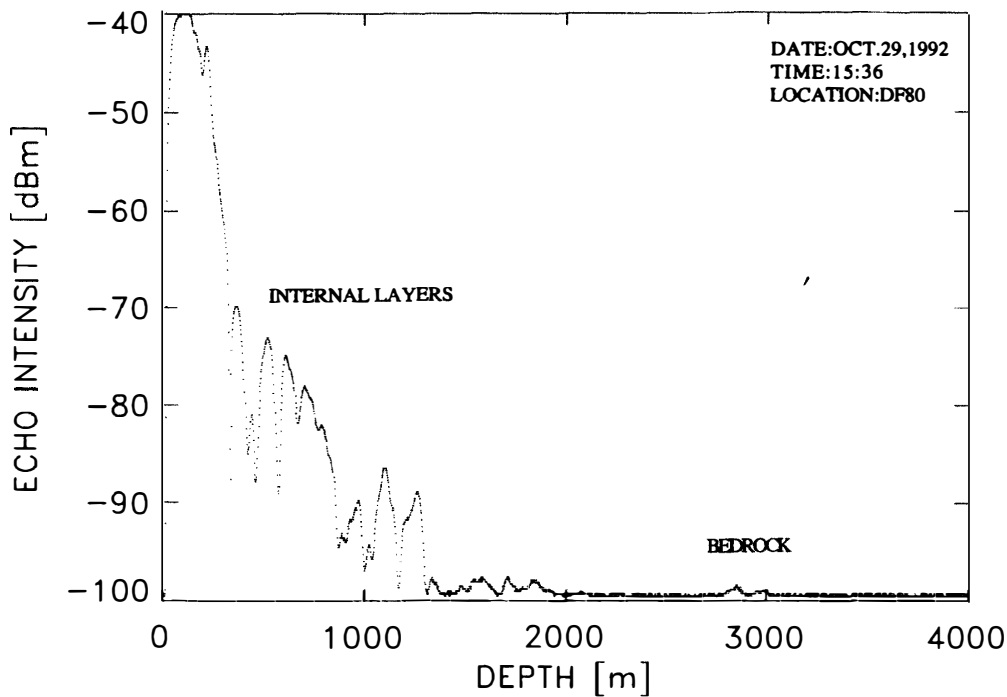


Fig. 3. Sample A-scope image.

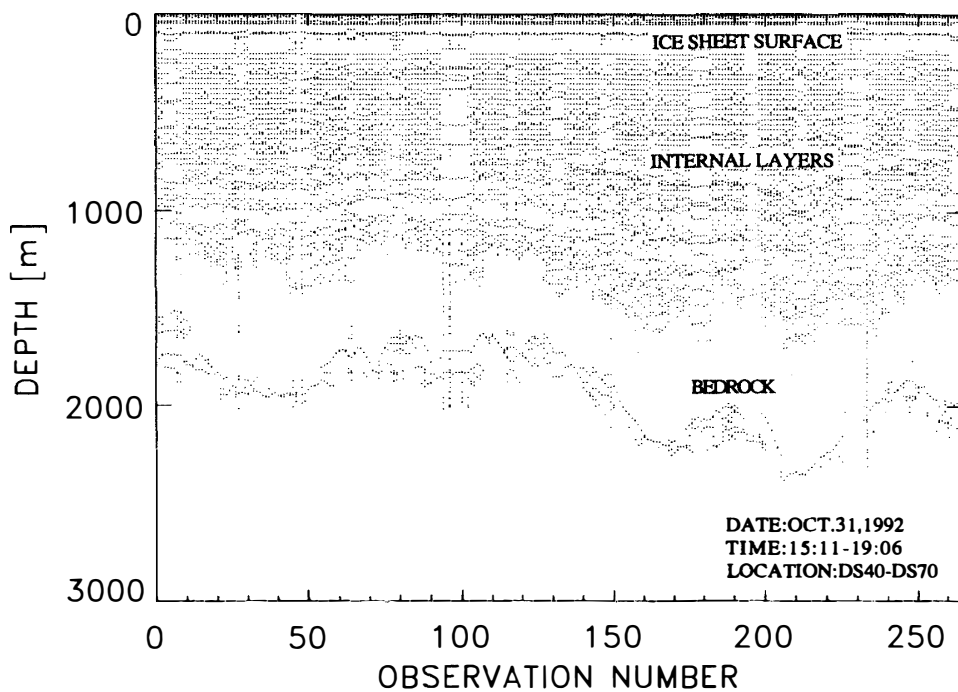


Fig. 4. Sample Z-scope image.

3. Observations

Figure 5 shows the route along which the mobile radio echo sounder was operated. The route stretched from a point called S16, about 15 km east of Syowa Station, via Mizuho Station, to the top of the Dome-F area. The total distance is about 1000 km. Station MD732 (3810 m above sea level), about 10 km north of station DF80, is the point of maximum surface elevation in the Dome-F area.

The longitude and latitude of observation were determined precisely by using GPS (Global Positioning System) signals. The surface elevations were also calculated from GPS signals and calibrated by the barometric measurements

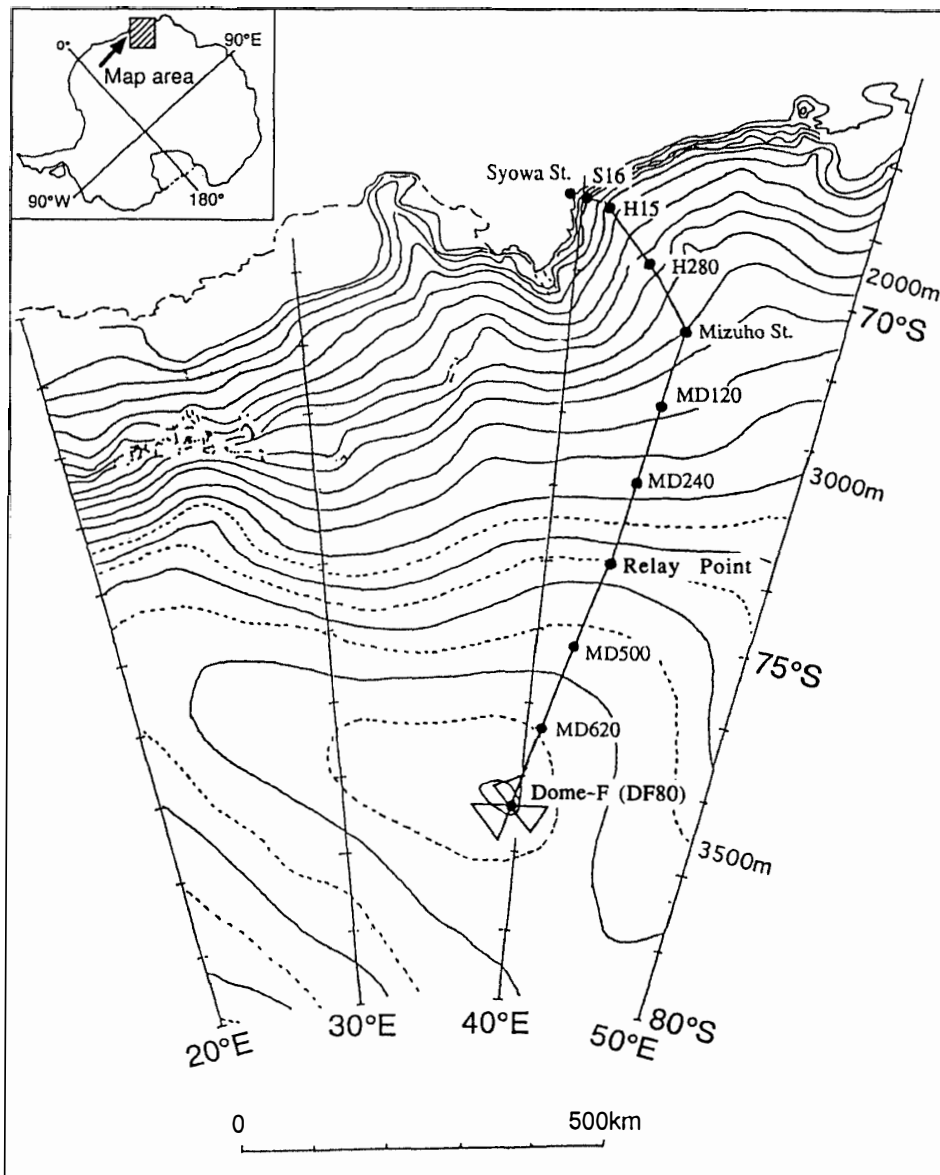


Fig. 5. Route map of the JARE-33 traverse. Each solid circle shows the location of the main observation point. Each name (such as MD240) indicates the point name.

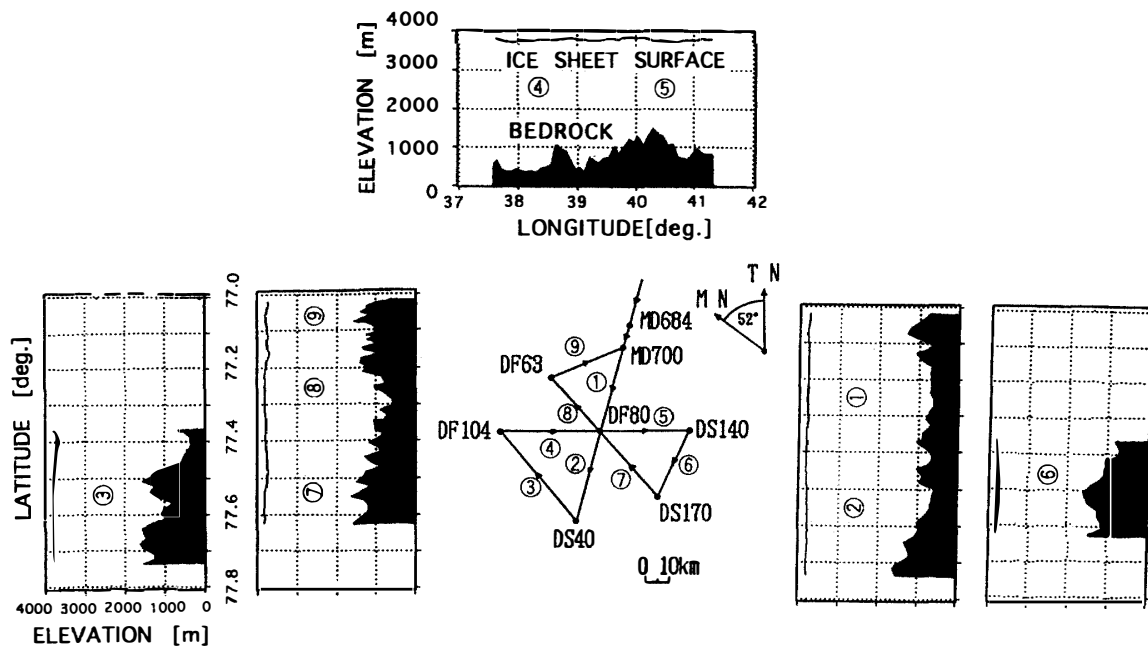


Fig. 6. The surface and bedrock elevations along the route around the Dome-F area.

performed at several locations around the observation points (KAMIYAMA *et al.*, 1994). Radio echo soundings were made only during the return trip from Dome-F to S16 from October to December, 1992.

Around the Dome-F area, the more precise radio echo observation was performed in a continuous manner along the routes shown in Fig. 6. The longest line was about 70 km, and the total observation time in the Dome-F area was about one month in October and November. The elevation of the Dome-F area is about 3800 m; the average air temperature was about -45°C during the observations.

4. Results

4.1. Bedrock topography

Figure 6 shows the surface elevations and bedrock elevations in the Dome-F area along each line (from No. 1 to No. 9). Echoes from the bedrock were judged from A-scope images every 2 km. The bedrock was always detectable, and the ice sheet was more than 2 km deep everywhere. The bedrock topography was found to have a basin-like shape; the bedrock elevation around DF80 was near its minimum in the Dome-F area. The elevation contour lines in the Dome-F area are shown in Fig. 7.

Figure 8 shows the observed bedrock elevations along with the routes between Dome-F and S16. There were several areas where the return signal from the bedrock was too weak to be detected. As indicated by arrows in Fig. 8, these areas were located around 69.6°S , 70.5°S , and 72.2°S . Return signals from internal layers in the ice sheet were also weak in these areas.

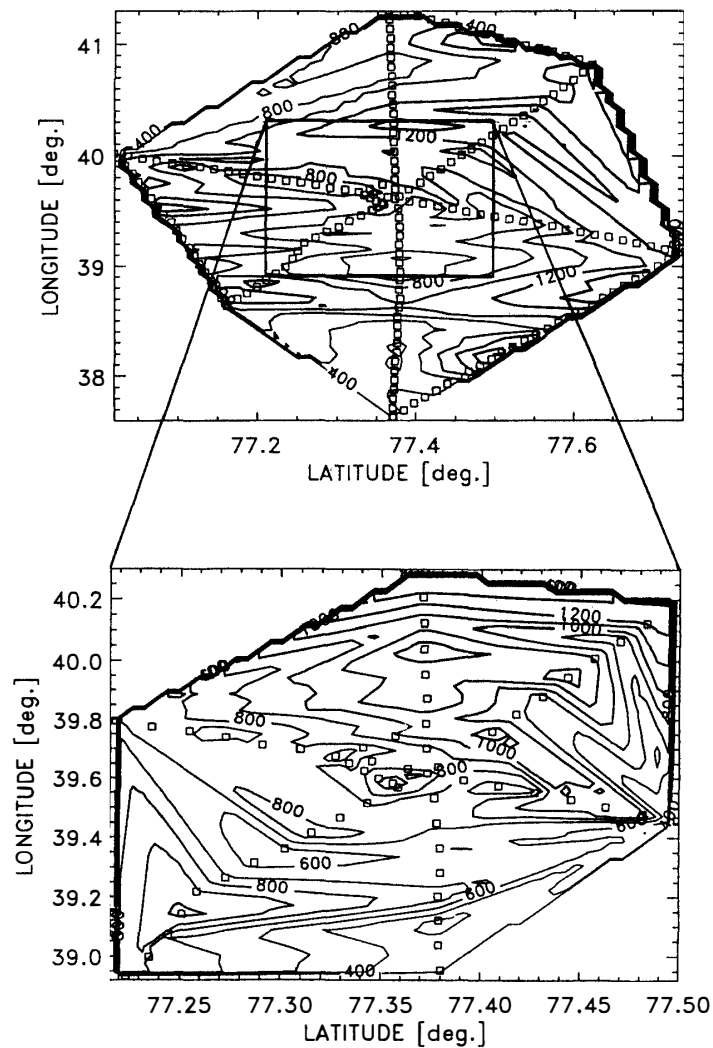


Fig. 7. The bedrock topography around the Dome-F area.

4.2. Performance of the radio echo sounder as an ice thickness detector

The maximum bedrock echo depth reached 3500 m of ice thickness, which is deeper than the expected 2900 m depth calculated from the JARE-27 results. The power received from the bedrock (relative to noise level) *versus* ice thickness is shown in Fig. 9. Up to about 2 km in ice thickness, the received power decreases with increase in ice thickness. For example, the received power at 500 m thickness is about 40 dB, while at 1500 m it is about 10 dB. The round-trip attenuation in the ice is about 30 dB/km. The nearly constant rate of decrease indicates that the attenuation in the ice sheet is the major factor causing signal attenuation, although there is some ambiguity due to the scattering cross section of the bedrock itself. When the thickness is more than 2 km, however, the received power scatters considerably and in some cases, the return power from the bedrock through a thicker ice sheet appears stronger than that through a thinner sheet.

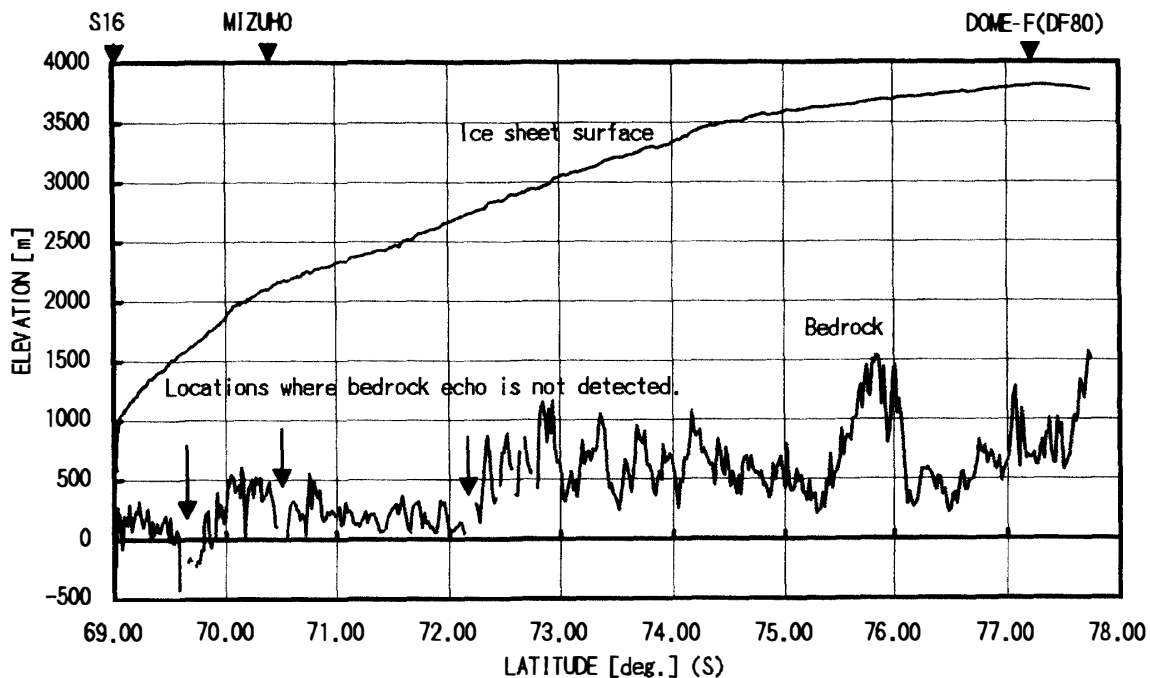


Fig. 8. Observed bedrock elevations along the route from S16 to Dome-F.

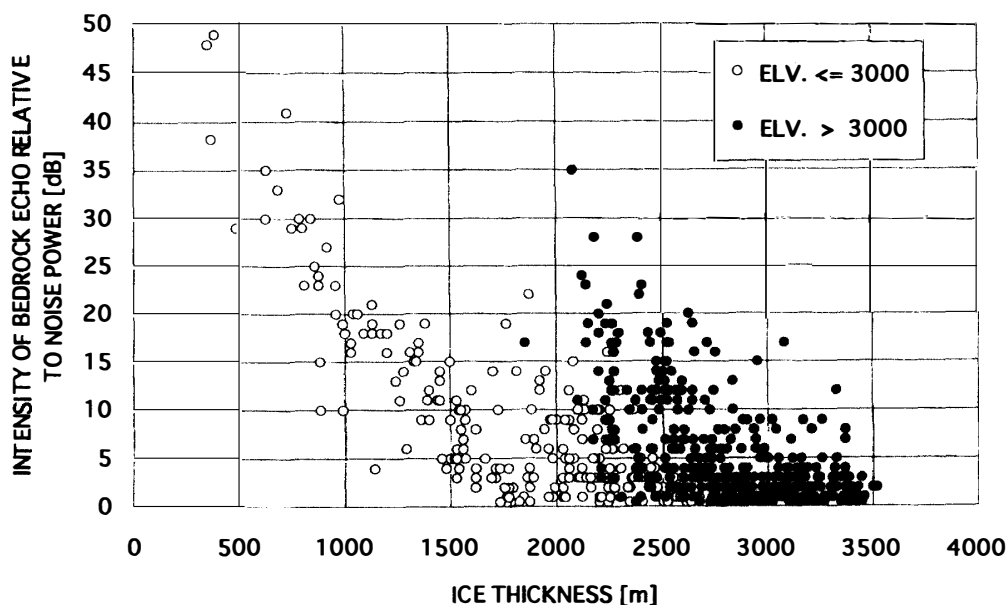


Fig. 9. Received power from the bedrock (relative to the noise level) vs. ice thickness. The data obtained at the points where the surface elevations are below 3000 m asl are shown by open circles, and those above 3000 m asl in solid circles, respectively.

Strong return signals were received from the bedrock mainly in the Dome-F area where the elevations are high. One of the reasons may be the lower ice sheet temperature, since the radio wave attenuation in ice decreases at lower temperatures (FUJITA, 1992). Laboratory experiments have shown that the

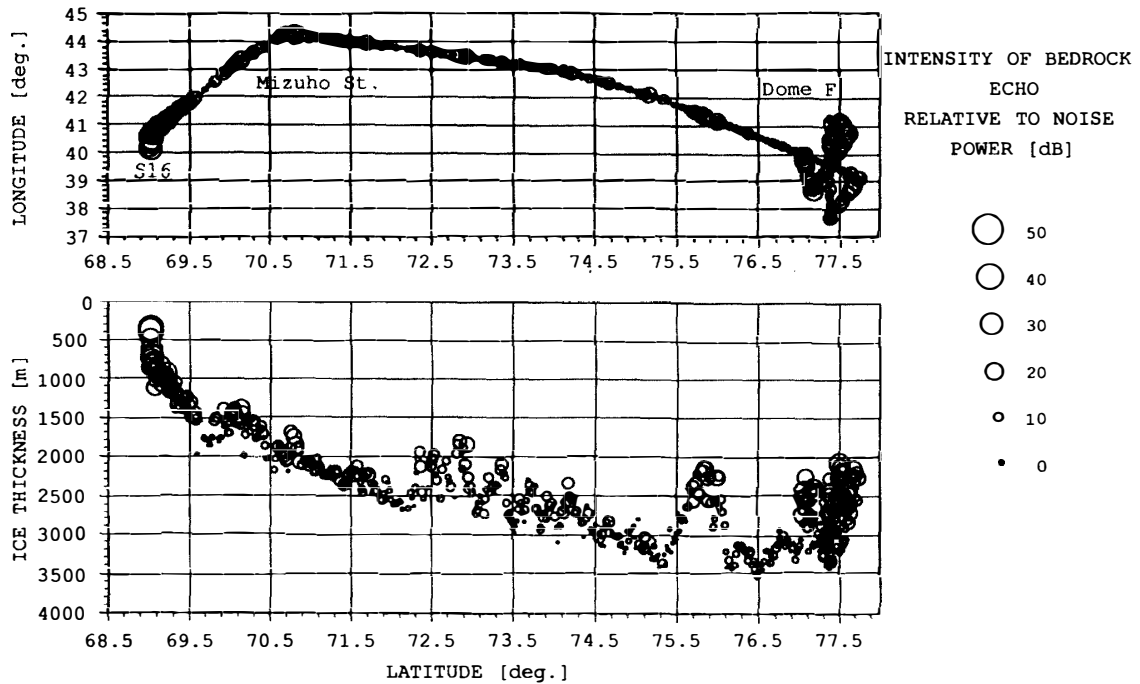


Fig. 10. The distribution of received power from the bedrock.

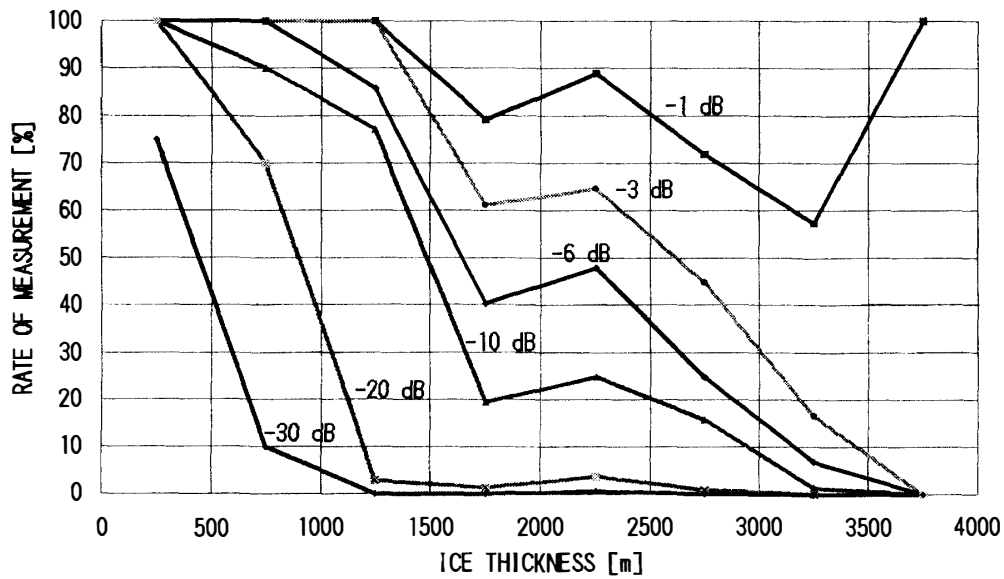


Fig. 11. Rate of bedrock detectability as a function of ice thickness for different transmitting powers.

temperature dependence of the radio wave attenuation is very large. For example, at -5°C and pH 6.0, the penetration depth for a signal with a frequency of several hundred MHz is about 120 m, which corresponds to 35 dB/km (FUJITA, 1992). Since the radar radio wave is attenuated on both legs of the round-trip, the attenuation becomes 70 dB/km. At -15°C , on the other hand, the round-trip attenuation becomes about 43 dB/km. This large difference of 27 dB indicates

the strong dependence of the attenuation on the ice temperature. This strong temperature dependence of the attenuation may explain the strong return signal from the bedrock at the Dome-F area. And the 30 dB/km attenuation indicates that the ice sheet temperature was less than -15°C , and even lower. The intensity of the return signal is shown at every point in Fig. 10. In the Dome-F area, the intensity is comparatively high against the ice thickness and decreases rapidly with increase of ice thickness.

The bedrock detection rates for several reduced transmitting powers are shown in Fig. 11 as a function of ice thickness. For example, if we use only half the peak power (-30 dB) of the current sounder, the bedrock detection rate is about 60% at an ice thickness of 2000 m. Generally speaking, the sensitivity of our radio echo sounder is good enough to detect bedrock more than 3000 m deep. If the peak power is reduced to less than a tenth that of the current system, however, the bedrock detectability decreases significantly at ice thicknesses greater than 1500 m. The performance seems to improve at ice thicknesses of about 2250 m. This is due to the strong return echo from the bedrock in the Dome-F area. The sharp increase of the rate-vs.-thickness curve for -1 dB from 3250 m to 3750 m is not reliable because only one data point was available at 3750 m.

4.3. Remote sensing of ice bodies

In the area below 3000 m asl, the round-trip attenuation in the ice was found to be about 30 dB/km, which, however, depends on the ice to some extent. In the area above 3000 m asl, the round-trip attenuation coefficient scatters substantially and cannot be determined. If the attenuation coefficient is determined in a specific area by the ice thickness-intensity relationship, the variation of ice characteristics may be detectable. The disappearance of the bedrock echo shown in Fig. 8 may possibly be due to the large radio wave attenuation in the ice sheet, because the ice in these areas seemed to be not very thick and the ice sheet temperature was not very low. The possibility to obtain the regional distribution of the attenuation in ice is shown in Fig. 10. This will be discussed more fully in a future paper.

5. Concluding Remarks

Using a radio echo sounder, operated as part of the Dome-F Project, the bedrock topography around the Dome-F area was obtained in a continuous manner. These measurements shows that Dome-F is located on bedrock basin surrounded by elevated areas.

The data will be valuable for the selection of a drill site for the Dome-F Project. The most suitable point may be the center of the Dome-F area, since the horizontal movement of the ice there is considered to be very low.

Bedrock topography was successfully measured under ice sheets more than 3500 m deep, and the performance of the radio echo sounder was confirmed.

The radio wave attenuation appeared to differ considerably between inside

and outside the Dome-F area. This difference seems to be due to the attenuation difference caused by the difference in ice temperatures.

Acknowledgments

We thank Prof. M. FUKUCHI, the leader of the wintering party, and the members of JARE-33.

References

- AGETA, Y., KIKUCHI, T., KAMIYAMA, K. and OKUHIRA, F. (1985): Ice thickness along the routes. JARE Data Rep., **125** (Glaciology 14), 6–29.
- FUJITA, S. (1992): Measurement on the Dielectric Properties of Ice at Microwave Frequency and its Applications to the Remote Sensing of the Polar Cryosphere. Hokkaido University, D. Sc. thesis.
- KAMIYAMA, K., FURUKAWA, T., MAENO, H., KISHI, T. and KANAO, M. (1994): Position, elevation, ice thickness and gravity. JARE Data Rep., **194** (Glaciology 21), 4–29.
- URATSUKA, S. (1990): Radio Scattering Characteristics of Antarctic Ice Sheet Using Airborne Radio Echo Sounding. Hokkaido University, D. Sc. thesis.
- URATSUKA, S., NISHIO, F., OHMAE, H. and MAE, S. (1989): Radio scattering characteristics of Antarctic ice sheet using airborne radio echo sounding data. Proc. NIPR Symp. Polar Meteorol. Glaciol., **2**, 142–151

(Received December 22, 1993; Revised manuscript received July 25, 1994)